Quality assurance of a helical tomotherapy machine

Article *in* Physics in Medicine and Biology · August 2004

DOI: 10.1088/0031-9155/49/13/012 · Source: PubMed

11 authors, including:

John D Fenwick
University of Oxford
123 PUBLICATIONS **1,975** CITATIONS
SEE PROFILE

Wolfgang Axel Tome
Albert Einstein College of Medicine
487 PUBLICATIONS **10,247** CITATIONS
SEE PROFILE

Hazim Ahmed Jaradat
University of Tabuk
61 PUBLICATIONS **1,223** CITATIONS
SEE PROFILE

Susanta Hui
City of Hope National Medical Center
177 PUBLICATIONS **3,304** CITATIONS
SEE PROFILE

Quality assurance of a helical tomotherapy machine

2004 Phys. Med. Biol. 49 2933

(http://iopscience.iop.org/0031-9155/49/13/012)

INSTITUTE OF PHYSICS PUBLISHING PHYSICS IN MEDICINE AND BIOLOGY

Phys. Med. Biol. **49** (2004) 2933–2953 PII: S0031-9155(04)71892-8

Quality assurance of a helical tomotherapy machine

J D Fenwick[1,2], W A Tomé[1,2], H A Jaradat[1], S K Hui[1], J A James[2], J P Balog[2,3], C N DeSouza[3], D B Lucas[3], G H Olivera[2,3], T R Mackie[1,2,3] and B R Paliwal[1,2]

[1] Department of Human Oncology, University of Wisconsin-Madison, 600 Highland Avenue, Madison, WI 53792, USA
[2] Department of Medical Physics, University of Wisconsin-Madison, 1300 University Avenue, Madison, WI 53706, USA
[3] Tomotherapy Incorporated, 1240 Deming Way, Madison, WI 53717, USA

E-mail: fenwick@humonc.wisc.edu

Received 11 November 2003, in final form 3 March 2004
Published 17 June 2004
Online at stacks.iop.org/PMB/49/2933
doi:10.1088/0031-9155/49/13/012

Abstract

Helical tomotherapy has been developed at the University of Wisconsin, and 'Hi-Art II' clinical machines are now commercially manufactured. At the core of each machine lies a ring-gantry-mounted short linear accelerator which generates x-rays that are collimated into a fan beam of intensity-modulated radiation by a binary multileaf, the modulation being variable with gantry angle. Patients are treated lying on a couch which is translated continuously through the bore of the machine as the gantry rotates. Highly conformal dose-distributions can be delivered using this technique, which is the therapy equivalent of spiral computed tomography. The approach requires synchrony of gantry rotation, couch translation, accelerator pulsing and the opening and closing of the leaves of the binary multileaf collimator used to modulate the radiation beam. In the course of clinically implementing helical tomotherapy, we have developed a quality assurance (QA) system for our machine. The system is analogous to that recommended for conventional clinical linear accelerator QA by AAPM Task Group 40 but contains some novel components, reflecting differences between the Hi-Art devices and conventional clinical accelerators. Here the design and dosimetric characteristics of Hi-Art machines are summarized and the QA system is set out along with experimental details of its implementation. Connections between this machine-based QA work, pre-treatment patient-specific delivery QA and fraction-by-fraction dose verification are discussed.

1. Introduction

Helical tomotherapy has been developed at the University of Wisconsin (UW) over several years (Mackie *et al* 1993, 1999), and commercial 'Hi-Art II' clinical machines are now manufactured by Tomotherapy Inc (Madison, WI). Tomotherapy delivers a rotating intensity-modulated fan beam of radiation, the modulation varying with gantry angle. Because the resulting dose-distributions comprise modulated contributions from many angles, the system has the potential to deliver highly conformal treatments (Reckwerdt *et al* 2000).

Axial, or serial tomotherapy (Low *et al* 1998a, 1998b, 1999) delivers dose-distributions slice-by-slice, patients being sequentially and discretely translated through the gantry rotational plane of a linear accelerator (linac) between slice deliveries. Helical tomotherapy on the other hand continuously translates patients through the bore of the machine as the gantry rotates, the therapy equivalent of spiral computed tomography (Kalender and Polacin 1991). This approach requires synchrony of gantry rotation, couch translation, linac pulsing and the opening and closing of the leaves of the binary multileaf collimator (MLC) used to modulate the radiation beam. Whereas axial tomotherapy can be accomplished by adding a binary MLC to the front of a conventional linac and moving the treatment couch using a highly precise indexing system, the helical approach has required a completely re-engineered machine—because to achieve continuous beam rotation many major system components have to be placed on a ring-gantry, coupled to the remaining non-rotating components (electrical power and high-pressure air supplies, static control and off-board computers) using slip-ring technology.

In the course of clinically implementing helical tomotherapy at the University of Wisconsin Comprehensive Cancer Center, we have developed a quality assurance (QA) system for our Hi-Art machine, building on the 'TG40' conventional linac QA schedule (AAPM Topic Group 40—Kutcher *et al* 1994) and previously described axial tomotherapy QA methodologies (Low *et al* 1998a, 1998b, Woo *et al* 2003). Here our system is set out, together with its rationale in the form of a review of the design and dosimetric characteristics of Hi-Art machines. Because these devices differ from conventional commercial linac systems (elements of the dose delivery being highly synchronized and dynamic), the QA system that has been set up contains some novel components. Experimental details of its implementation are provided, together with some baseline data and suggestions for modification of the system as the technology matures.

2. Rationale for the helical tomotherapy QA system

2.1. The helical tomotherapy process

Much has been published elsewhere detailing the design and dosimetry of Hi-Art machines (Balog *et al* 1999a, 1999b, 2003a, 2003b, Mackie *et al* 1993, 1999). These ideas are summarized here, and lead naturally to the QA system that has been implemented.

Figures 1 and 2 convey the essence of the dose delivery. A short in-line 6 MV linac (Siemens Oncology Systems, Concord, CA) rotates on a ring-gantry, at a source–axis distance (SAD) of 85 cm, whilst a patient-support couch is translated in the y-direction (IEC, 1996) through the gantry bore. Thus, in the patient's reference frame the beam is angled inwards along a helix, with the midpoint of the fan beam passing through the centre of the bore. The pitch (defined as the distance travelled by the couch per gantry rotation, divided by the field width in the y-direction) is typically 0.2 to 0.5. The y-width of the beam is defined by a pair of jaws and is fixed for any particular patient treatment to one of several selectable values,

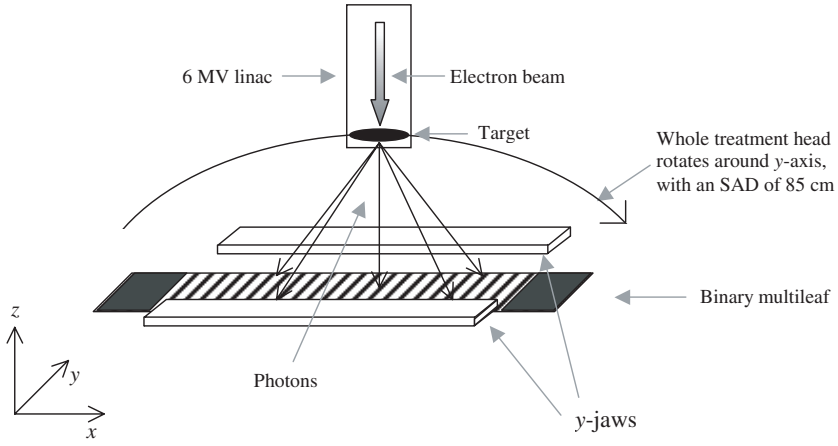

Figure 1. A simplified schematic of the Hi-Art treatment head pictured at a gantry angle of 0°, together with the IEC coordinate system. X-rays produced by a 6 MV linac are collimated down to a fan beam by a pair of jaws, and modulated laterally by a binary multileaf which is blocked off at both ends.

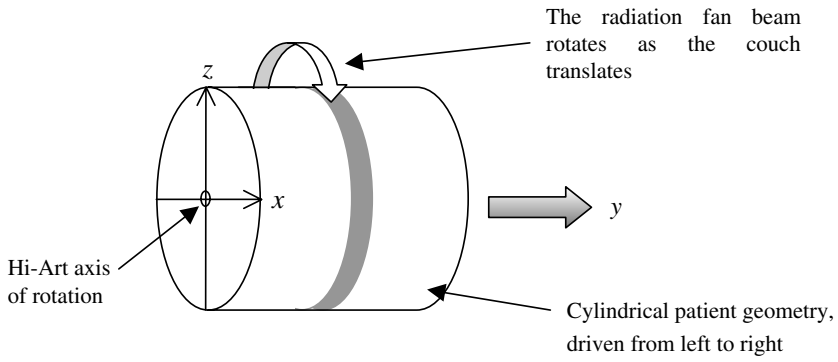

Figure 2. The Hi-Art fan beam axially rotates while the patient (pictured here as a cylinder) is translated along the axis of the machine by the moving couch.

for instance 1, 2.5 or 5 cm. Laterally the beam is modulated by a 64 leaf binary MLC (whose leaves transition rapidly between open and closed states), each leaf having a width of 6.25 mm projected to isocentre for a maximum possible open lateral field length of 40 cm. The system does not include a physical flattening filter. Consequently its dose-rate is increased, thus reducing treatment times (Deasy *et al* 2001), and the primary fluence emanating from the treatment head is forward peaked until it is modulated by the MLC (Balog *et al* 2003a).

Intensity modulation is accomplished by varying the fraction of time for which different leaves are opened. The modulation can change with angle, an individual modulation pattern being defined over the course of a 'projection' which corresponds to a gantry rotation of just over 7°, giving exactly 51 projections per revolution. The gantry rotates at a constant velocity during treatment with a period between 10 and 60 s per rotation, and so the time-per-projection is 196 ms or greater. The extent to which a projection is modulated can be characterized through the 'modulation factor'—the ratio of the maximum to the average leaf open time for the projection (the averaging excluding leaves beyond the projection's field edge, which do

not open). The maximum permissible modulation factor for any part of a delivery is specified during treatment planning; for complex geometries more highly modulated treatments achieve greater conformality but they inevitably take longer to deliver and are unnecessary for less complex cases.

2.2. Factors impacting on dose-distributions delivered by a helical tomotherapy machine

Helical tomotherapy is a highly dynamic treatment process whose accuracy depends on the correct performance of the radiation source, MLC, gantry and table. The total dose delivered to any anatomic site within a patient is, of course, the time-integral of the dose-rate at that site and thus depends on factors relating to

(1) static beam dosimetry;
(2) system dynamics;
(3) system synchrony;
(4) system geometry.

The static beam (1) and geometric (4) groups of factors are similar to those determining dose-distributions delivered using conventional linear accelerators. Dynamic (2) and synchrony (3) factors have some overlap with similar aspects of sliding window IMRT and axial tomotherapy system performance (LoSasso *et al* 1998, Low *et al* 1998a, 1998b). In total we have identified 23 machine characteristics (factors (a)–(w) detailed below) that impact on delivered dose.

2.2.1. Static beam factors. The static beam factors that lie at the heart of helical tomotherapy dosimetry (Balog *et al* 2003b) are

(a) output, characterized as dose-rate at some depth in water for a fixed field-size with the source–surface distance (SSD) set at the Hi-Art SAD;
(b) field-size dependent output factors;
(c) off-axis profile in the lateral direction measured at some depth in water;
(d) off-axis profile in the *y*-direction measured at some depth in water;
(e) depth-dose variation, characterized as a percentage-depth-dose in water for a fixed field-size;
(f) output ramp-up time and subsequent stability.

These factors differ a little from their conventional linac equivalents. Firstly, Hi-Art machines do not work on a monitor unit-based system, but operate more like a cobalt unit. Output (a) is therefore calibrated in terms of a reference dose rate, measured in units of cGy per minute rather than the conventional cGy per monitor unit.

Secondly, because Hi-Art machines do not have flattening filters, the head scatter contribution to dose is lower than that of conventional linacs (Chaney *et al* 1994). This allows the variation of output factor with field-size (b) to be adequately modelled in three stages:

(bi) changes in head scatter with jaw setting are accounted for by modelling independent output factors for each of the jaw settings selectable for patient treatments;
(bii) the variation of phantom scatter with the extent of field irradiated is dealt with by the convolution-based dose calculation algorithm of the planning system;
(biii) the remaining factor significantly impacting on output is the tongue-and-groove (TG) effect (Balog *et al* 1999b), which causes an increase in the fluence-per-leaf-opening if many neighbouring leaves are opened together, compared to that when only one or a few neighbouring leaves are opened. It is corrected for by the planning system, which

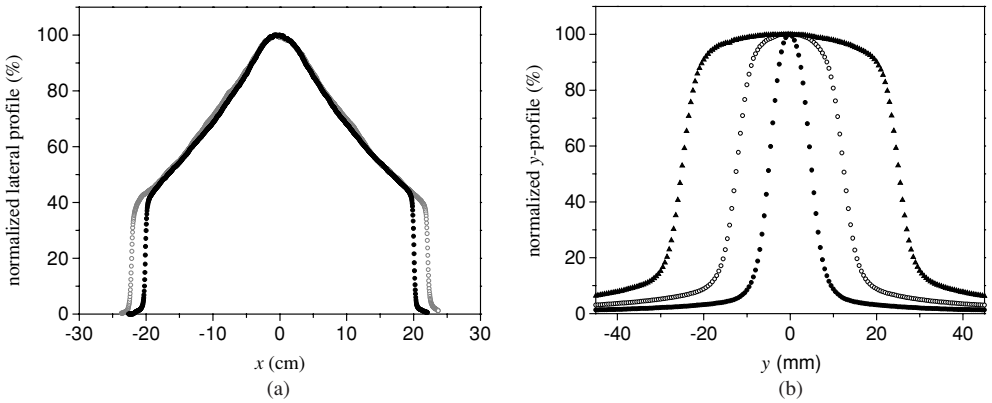

Figure 3. (a) Lateral profiles measured for a 40 × 2.5 cm^2 field at an SSD of 85 cm and depths in water of 1.5 (●) and 10 cm (○); the profiles have been normalized to 100% on the central axis. (b) *y*-axis profiles (normalized to 100% on the central axis) measured for 40 × 1 (●), 40 × 2.5 (○) and 40 × 5 cm^2 (▲) fields at 10 cm depth in water along the axis of the Hi-Art machine.

multiplies planned leaf opening times by TG correction factors measured at machine commissioning. These TG factors are specific to each leaf, and are determined by measuring the fluence-per-leaf-opening when only an individual leaf is opened and then comparing this value to those measured when the leaf plus either or both of its neighbouring leaves are opened together (Balog *et al* 2003b).

Thirdly, the forward peaking of the primary radiation beam is reflected in the shape of the lateral profile (c), while the shape of the *y*-profile (d) is mainly determined by the jaw opening and penumbra width (figure 3). Historically, beams produced by conventional treatment units were intended to be uniformly flat and symmetric to accommodate treatment with broad unmodulated beams. However, this constraint is unnecessary for helical tomotherapy because the lateral profile is modulated by the MLC and the static *y*-profile is smeared out by the helical delivery. Thus classical measures of the off-axis dose-distribution such as flatness and symmetry are not very relevant. Of course, it is important that the profile shapes measured at commissioning (Balog *et al* 2003b) and modelled by the Hi-Art planning system accurately reflect machine performance at the time of treatment. This is particularly critical when treating patients set up with their midlines roughly centrally located in the Hi-Art bore but with targets lying off midline, as the dose delivered to such offset targets will depend heavily on the shape of the lateral profile.

Fourthly, depth-dose variation (e) is typically rather greater than that of conventional 6 MV machines because of the reduced Hi-Art source–axis distance (Balog *et al* 2003a). And finally, output ramp-up time (f) is the interval from the commencement of linac pulsing to the point where output reaches a stable value (figure 4(a)). To allow the dose-rate to stabilize before beginning a patient treatment, the MLC is kept closed for a fixed time after the start of linac pulsing, which clearly should be at least as great as the ramp-up time. After ramp-up, beam stability over the course of a treatment (typically a few minutes) is essential for accurate dose delivery, and is therefore monitored by an interlock system that terminates treatment if the output averaged over 1 and 5 second windows deviates from the reference level by more than 50% or 5%, respectively. In fact stability is generally substantially better than this. Pulse-by-pulse output data collected over 2 minutes for a helical delivery with a 12 s gantry rotation

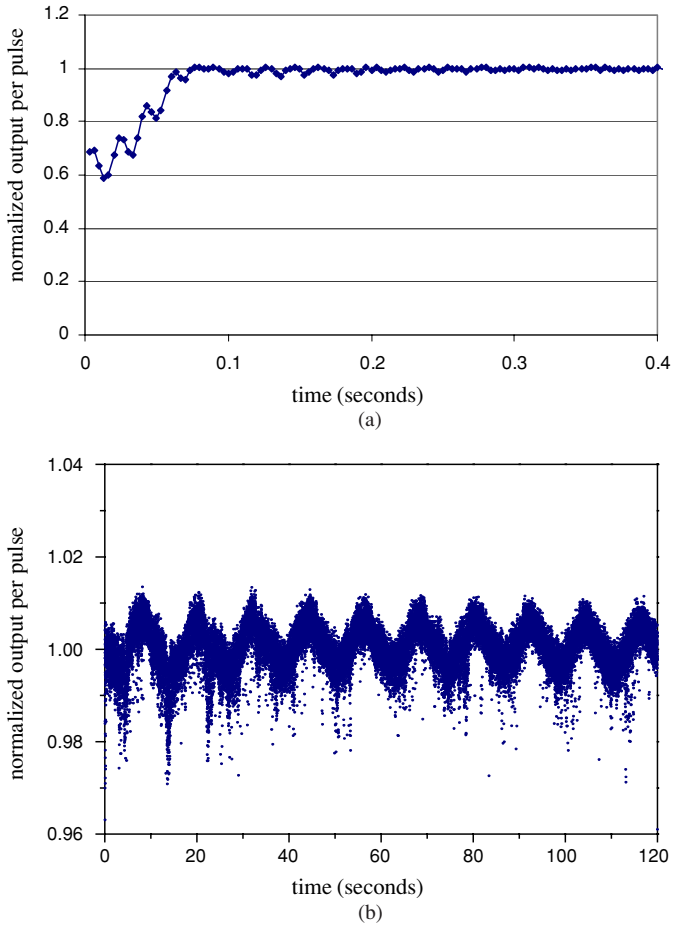

Figure 4. (a) Ramp-up of output from the Hi-Art machine, measured as the pulse-by-pulse signal from one of the dose-rate monitoring ion chambers in the machine head. Output is normalized to the long-term average. (b) Hi-Art pulse-by-pulse data collected over 2 min for a helical delivery with a 12 s gantry rotational period.

are shown in figure 4(b). Other than a small periodic variation (which occurs because the output-per-pulse depends slightly on gantry angle), the output is very stable.

2.2.2. System dynamics. To first order, the total dose delivered to a point in a patient's highly irradiated target volume varies linearly with the length of time for which the point lies within the Hi-Art fan beam (Fenwick and Tomé 2004). For such a point (one irradiated from a large range of gantry angles) this time depends on the dynamic factors:

(g) width of the field in the *y*-direction (defined by the jaws);
(h) couch velocity;
(i) 'actual' fraction of time for which the leaves are open (programmed fraction × latency factor).

Field width (g) is both a geometric factor (impacting on the superior and inferior borders of treated high dose regions—section 2.2.4.) and a dynamic factor. When a patient is transported

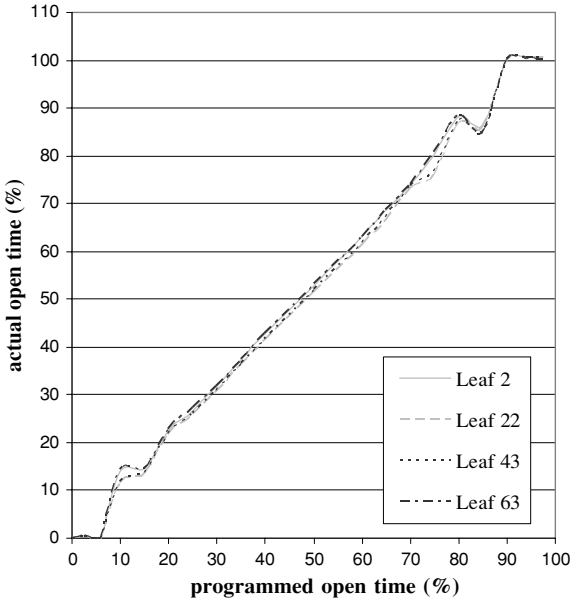

Figure 5. A plot of 'actual' versus programmed open times for a Hi-Art multileaf, measured for four different leaves and a 200 ms projection time.

though the beam lying on the treatment couch, the time for which a point within the patient's target volume lies in the radiation field varies linearly with the width of the field and inversely with the couch speed (factor (h)). This mirrors the dependence on window width and leaf velocity of the length of time for which a point is irradiated by a sliding window IMRT field (LoSasso *et al* 1998).

The ways in which delivered dose depends on factors (a)–(e) and (g)–(h) are further elucidated elsewhere, for the fundamental case of a cylindrical phantom aligned coaxially with the Hi-Art machine and irradiated using helical deliveries with all leaves constantly open (Fenwick and Tomé 2004). Fractional leaf opening time (factor (i)) can be worked into the dosimetric framework without introducing any beam modulation, by considering the implications of opening all the leaves only for some fixed fraction of each projection time. The dose delivered scales linearly with 'actual' fractional open time, which differs from programmed open time because of 'leaf latency' effects (Tsai *et al* 2000, Kapatoes *et al* 2001b)—the finite opening and closing times of the leaves (around 20 ms for a Hi-Art system) and slight delays in control electronics. Consequently, programmed leaf open times are calculated by the tomotherapy planning software using a two stage process. Initially, 'actual' open times are calculated by the plan optimizer and then these times are empirically 'latency corrected' by the software to arrive at programmed open times that deliver the required fluence levels.

Latency corrections are determined at commissioning by measuring the background-subtracted fluence when a leaf is opened as a function of fractional programmed opening time and projection time. Dividing the signal measured for some fractional programmed open time by the 100% open time signal gives the corresponding 'actual' fractional open time. Plots of actual versus programmed open times measured for four different leaves and a 200 ms projection time are shown in figure 5. Such plots are roughly linear and do not change greatly from one leaf to another, and so the straight line relation:

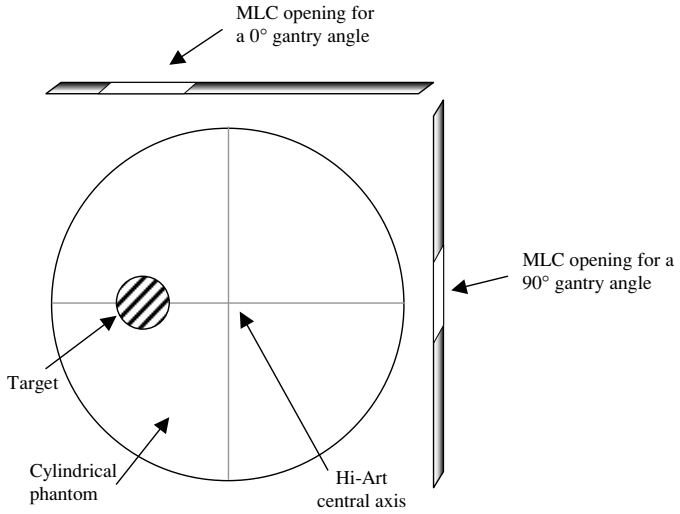

Figure 6. An illustration showing an offset target in a cylindrical phantom whose centre lies on the axis of a Hi-Art machine. The extent to which the target is offset from the central axis of the Hi-Art fan beam varies with angle, and so leaf opening must be correctly synchronized with gantry angle or dose will be delivered to incorrect locations.

$$\text{programmed fractional open time} = m(\tau_P) \times \text{actual fractional open time} + c(\tau_P) \quad (1)$$

(where τ_P is the projection time) is fitted to the average of the curves measured for different leaves (Balog *et al* 2003b). Equation (1) is used by the planning software to convert calculated to programmed open times. Latency effects increase with decreasing projection time, leaf opening and closing times constituting a significant fraction of the shortest projection times. Therefore latency data are measured and fitted for several different projection times, and the corrections actually applied to a treatment plan are generated by interpolating between the latency data fits obtained for those projection times closest to that of the plan.

2.2.3. System synchrony. If delivered dose-distributions are to match up with planned distributions, then in addition to controlling factors (a)–(i) several elements of the delivery must be synchronized with gantry angle—specifically:

(j) leaf opening;
(k) linac pulsing;
(l) couch drive.

The impact of factor (j) on delivered dose-distributions is illustrated in figure 6, which describes a treatment targeting an off-axis site. To keep the target continuously in the radiation field, the pattern of open leaves has to change with gantry angle otherwise dose will be delivered to incorrect locations. And so the Hi-Art machine locks leaf opening to gantry angle through a patented 'tick fence' which triggers a fixed number of feedback control pulses per degree of rotation, providing a measure of the total angle through which the gantry has turned.

Consider now the dose-distribution generated by a helical delivery with a 'loose' pitch (greater than 1). The target is irradiated from all angles and is thus continuously covered with a high dose. Beyond the lateral border of the target, however, the dose-distribution takes a shape resembling a spiral staircase, smoothed out by the continuous nature of the delivery (Fenwick and Tomé 2004). Generally helical tomotherapy is delivered with a 'tighter' pitch

(less than 1), contracting down the dose-distribution beyond the target so that the staircase overlaps itself. Beam divergence adds further structure to the distribution, generating a small 'thread' perturbation of dose within the target region (Kissick *et al* 2004).

If the linac were run at a fixed pulse repetition rate but the gantry rotation speed varied a little with angle (because of an imbalance of the gantry) then beyond the target the dose-levels around the peripheral spirals would also vary slightly with angle. This follows because dose would be roughly proportional to time spent in the beam, and beyond the border of the target region the time spent in the beam depends on the rotational speed of the gantry. Actually, pulsing of the linac (factor (k)) is also locked to gantry rotation though the tick fence, leading to a constant output per degree of rotation and removing the erroneous angular dose variation.

Couch velocity (factor (l)) is not yet locked to gantry rotation in the Hi-Art system; couch and gantry speeds are currently considered sufficiently independently well regulated to achieve adequate synchrony. In fact slight differences between the planned and actual speed of the couch relative to the gantry rotational velocity can arise because the Hi-Art tolerance on gantry rotation speed is 2% (although with precise calibration better accuracy can be achieved, at least initially). Such differences will lead to small dose delivery errors: a velocity mismatch of up to 2% would lead to all the rotations of a treatment being completed over 98–102% of the planned target length, creating inaccuracies of $\pm 2\%$ in the length of the highly dosed region (equivalent to a ± 2 mm uncertainty on the inferior border of a 10 cm long target) and in the dose-level delivered to the target. These errors can, and will, be eliminated by locking couch and gantry drive. Likewise, the shapes of the target region thread effect and the peripheral spiralling will be correctly calculated by the planning system if the couch and gantry are tightly synchronized, but otherwise will be a little distorted.

Given correct matching of average couch and gantry speeds, if the couch speed is constant, while the gantry speed varies a little with angle then a small periodic *y*-direction ripple will be generated in the target region dose-distribution. This dose variation occurs because the output (number of linac pulses) per angle is held constant, and so variations in gantry speed lead to fluctuations in the number of pulses per second. Elsewhere it is shown that for a typical pitch of 0.4, a variation of $\pm 1\%$ in gantry speed will lead to a *y*-direction ripple of $\pm 0.1\%$ in the target dose-distribution (Fenwick and Tomé 2004). An almost identical effect is created by rotational variation of the linac output per pulse (figure 4(b)), a $\pm 1\%$ output-per-pulse rotational variation also leading to a $\pm 0.1\%$ ripple for a pitch of 0.4.

2.2.4. System geometry. Given accurate beam dosimetry, system dynamics and synchrony, planned dose-distributions will be accurately delivered using the Hi-Art system provided that the machine geometry is set up to match the geometric design modelled by the planning system. Many innovative Hi-Art geometric checks have been described by Balog *et al* (2003a) including tests of

(m) field centring in the *y*-direction, checking that beams do not diverge out of the rotational plane of the gantry;
(n) collimator twist, checking that the jaws are aligned with the gantry plane;
(o) MLC twist, checking that leaves run perpendicular to the gantry plane;
(p) MLC centring and alignment, assessed by determining that the central leaves 32 and 33 project to either side of the isocentre, and that TG artefacts induced in the radiation beam lateral profile by sequentially opening neighbouring leaves are roughly symmetric about the field centre.

These checks are largely analogous to the testing of conventional linac jaw symmetry and collimator rotation angle. Additional geometric factors that should be tested include

(q) isocentre constancy with gantry rotation;
(r) gantry angle accuracy;
(s) jaw opening width (to ensure that superior and inferior target borders are accurate);
(t) laser set-up, checking that lasers point to the 'virtual isocentre' and are correctly aligned with the machine axes;
(u) couch top horizontal levelling;
(v) couch drive distance accuracies in the y- and vertical- (z-) directions;
(w) couch drive direction accuracy, checking that y-axis translations are perpendicular to the gantry rotational plane and that z-axis translations are unaccompanied by movement laterally.

These elements of the Hi-Art geometry impact on treatment delivery in similar ways to their conventional linac analogues, although a couple of differences exist. Firstly, the radiation isocentre lies within the Hi-Art gantry bore and because neither lasers nor patients can be practically set up there, the lasers instead point to a 'virtual' isocentre set at a fixed distance out (70 cm) along the y-axis from the radiation isocentre—an arrangement also used for CT simulators. Patients are set up to the virtual isocentre and then a couch shift translates them to the radiation isocentre.

Secondly, accurate couch drive is perhaps even more critical for helical tomotherapy than for conventional therapy. Treating conventionally, the couch moves made after setting up lasers to skin marks are typically fairly limited, whereas during a tomotherapy delivery there is a substantial couch drive to translate from the virtual to the real isocentre followed by a further drive over the length of the target volume. Inaccuracy of the drive from virtual to real isocentre is inherently tested for and corrected frequently by acquiring pre-treatment megavoltage computed tomography (MVCT) scans to check patient positioning. However, small inaccuracies in couch drive distance and orientation over the course of the translation through the length of the target will have consequences for the geometric accuracy of dose delivery, a 1° drive direction angular deviation in the x–y plane, for example, leading to lateral shifts of ± 1 mm at the superior and inferior borders of a 10 cm long target.

3. QA implementation techniques and some baseline data

3.1. A quality assurance schedule for helical tomotherapy

The current QA measurement schedule for the UW Comprehensive Cancer Center Hi-Art II machine is summarized in table 1. It is designed to systematically assess the factors catalogued in section 2.2. Tolerance values are also shown in the table and represent TG40-type action levels. Generally, the treatment system should be adjusted if a QA measurement is out of tolerance. However, it is currently more practical to deal with changes in certain machine characteristics (for example, output and leaf latency) by modifying the planning system dosimetric modelling to match the machine performance, rather than vice versa.

Two changes to the schedule are foreseeable in the near future. Firstly, monitoring of the lateral profile will become less frequent once the Hi-Art system is configured to interlock out in the event of any notable change in beam profile. Secondly, it is intended to make those checks currently scheduled three monthly on a less frequent basis (six monthly and then annually) once sufficient long-term experience has been gained to justify the change.

Table 1. A schedule of helical tomotherapy QA measurements.

	Daily checks
D1	Output constancy quick check (±2%)
D2	$TPR_{20/5}$ quick check (±2%)
D3	Lateral profile constancy quick check (±2%)
D4	Output ramp-up time (<10 s)
D5	Combined dosimetric check of jaw width, couch speed, leaf latency, output and (potentially) leaf/gantry synchrony (±2%)
D6	Lasers (±1 mm)
	Monthly checks
M1	Static output in reference geometry (±2%)
M2	Rotational stability of output (±2%) and lateral profile (±2%)
M3	Static output stability over 5 min (±2% for 30 s window-averaged output)
M4	Couch drive speed (±1%) and uniformity (±2% optical density profile variation)
M5	Leaf opening synchronized with gantry rotation (±1°)
M6	Couch *y*-translation per gantry rotation accurate over several rotations (±1 mm)
M7	Virtual isocentre (±1 mm)
M8	Gantry 0° (±.5°)
M9	Jaw width constancy (±1 mm)
	Three-monthly checks (likely to be made less frequent as experience is gained)
T1	Rotational stability of delivered dose (±2%)
T2	Leaf latency (±2%)
T3	Couch translation and gantry rotation synchronized throughout each rotation, and negligible output-per-pulse rotational variation (±2% on-axis dose ripple)
T4	Laser alignment (±.5°)
T5	Star film check of radiation isocentricity (±1 mm)
T6	Couch drive distance into bore and up/down (±1 mm)
T7	Couch drive into bore orthogonal to gantry plane (±1°)
T8	Couch drive up/down orthogonal to horizontal plane and parallel to gantry plane (±1°)
T9	Couch top flatness (±1°)
T10	Radiation field divergence out of gantry plane (±1 mm)
T11	Multileaf alignment (±1 mm)
T12	Jaw twist (±1 mm over whole 40 cm open field length)
T13	Multileaf twist (visually assessed)
T14	Field centre constancy with jaw size (±1 mm)
	Annual checks
A1	Depth-doses, lateral and *y*-axis profiles (±2%)
A2	Dose at the centre of a cylindrical phantom for various field sizes and numbers of rotations (±2%)
A3	Multileaf leakage (<1%)
A4	Tongue-and-groove effect factors (±1%)
A5	Output interlocking (±50% over 1 s, ±5% over 5 s)

3.2. Implementational details

3.2.1. Daily checks. Output constancy (daily check D1) is measured for a static 10×5 cm^2 field with 30 s of beam-on time, using an isocentrically located ion chamber placed 5 cm from the end of a 25 cm long cylindrical perspex 'quick check' phantom aligned with the lateral IEC *x*-axis of the machine, with the gantry set to 90°. The (temperature- and pressure-corrected) measurement is nominally related back to dose in water at d_{max} depth and an SSD of 85 cm

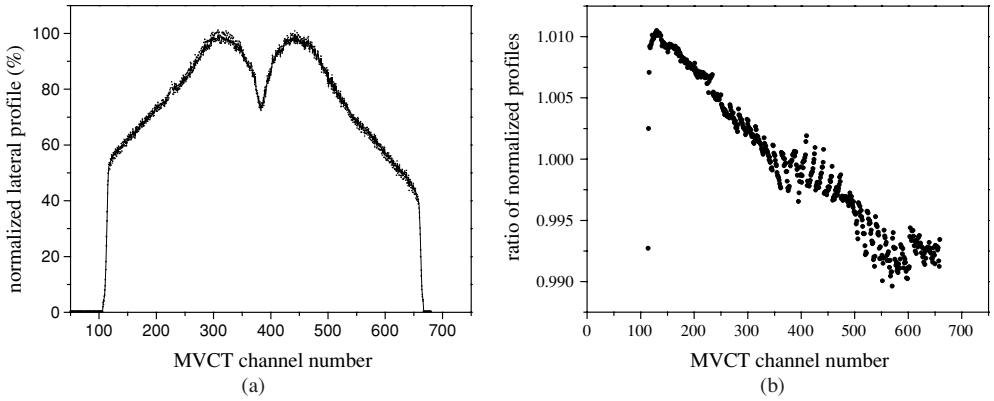

Figure 7. (a) The average (line) and limited range (dots) of normalized lateral profile shapes measured over the course of a rotating delivery using the MVCT array detector. The profile shape has a central dip embedded in it by the build-up characteristics of the detector. (b) The ratio of the average normalized lateral profile to an earlier reference.

through a pre-determined phantom factor. Energy constancy (check D2) is assessed using an approximation to the tissue phantom ratio (TPR) for depths of 5 and 20 cm. The approximate $TPR_{20/5}$ is determined by rotating the gantry to 270° so that the ion chamber lies at a depth of 20 cm in the perspex quick check phantom, and dividing readings for this orientation by those made with the gantry at 90°. This test can be rapidly carried out and provides a useful spot check (90° versus 270°) that output uniformity with gantry angle is invariant, as well as checking energy constancy.

Using an ion chamber placed at the centre of a cylindrical solid water phantom aligned coaxially with the Hi-Art machine, dose is also measured every day for a fully intensity modulated treatment (check D5), planned (using the Hi-Art treatment optimizer) to deliver a dose of 2 Gy to a target of y-direction length 10 cm. The modulation factor of 2.2, 20 s rotation period and 0.4 pitch of the delivery are representative of typical treatments. The 2.5 cm jaw width selected is that currently used for curative (mostly prostate) treatments on our machine. The measurement can be made reasonably quickly and is a check of the combined impact of jaw width, couch speed, leaf latency and static beam dosimetric inaccuracies on delivered dose. Working with a planned target cross-section that is wide in the x-direction but narrow in the z-direction, and measuring the delivered dose both at isocentre and at 10 cm off-axis, this test can also provide a rough daily check of MLC synchronization with gantry angle: any significant MLC/gantry asynchrony would substantially change the off-axis delivered dose. A more precise synchrony test is provided by monthly check M5.

The shape of the lateral profile (check D3) is captured for a 40×1 cm^2 field static delivery using the Hi-Art's integrated MVCT detector system (Mackie *et al* 1993, Balog *et al* 2003a), data from which is written to a file. The build-up characteristics of the detector embed a central dip in the profile (figure 7(a)) and so this test is not used to assess the absolute profile shape, but rather to check its constancy by plotting the ratio of the newly acquired profile (retrieved from a file created by the MVCT system) to a reference profile obtained at commissioning.

Signals from the Hi-Art dose-monitoring ion chambers are stored along with the MVCT data; and using the signal from one of the chambers, a plot is generated of the rise in output after beam switch-on against time (figure 4(a)). The plot is visually assessed (check D4) to ensure that the output from the linac rapidly ramps up to its maximum value; it must do so

within 10 s, as this is the (adjustable) interval for which all leaves are currently kept closed at the beginning of each treatment.

A laser set-up to the virtual isocentre (check D6) is conveniently tested every day using the SonArray optical guidance system (ZMed, Ashland, MA). A jig is lined up to the lasers, and the guidance system then provides a comparison of the jig location with a fixed reference point (the virtual isocentre) established at machine commissioning. In the absence of optical guidance any alternative fiducial mark could be used instead—for example, a reference point on the couch, at a fixed couch position.

3.2.2. Monthly checks. Output is measured directly at 5 cm deep in water with an SSD of 85 cm (check M1) using an ion chamber placed at the centre of a 5×10 cm^2 field, irradiated for 30 s. The reading is linked back to dose at $d_{\max}$ through a PDD curve measured at commissioning.

Rotational beam stability (check M2) is determined using the Hi-Art's on-board MVCT detector array. A rotational treatment is delivered with all leaves open, a jaw width of 1 cm and the couch retracted out of the bore. The MVCT detector captures the shape of the lateral beam profile at each linac pulse. The pulse-by-pulse Hi-Art ion chamber measurements stored alongside this profile data are plotted to characterize the variation of output with gantry angle, generating a trace like the first 30 s of figure 4(b). The angular output variation shown by such traces correlates well with dose measurements made at isocentre for a fixed delivery time and a range of (static) gantry angles.

Normalized lateral profile shapes are determined for each pulse; the normalized profile value at a point being calculated as the ratio of the detector reading at that point to the totalled array signal for that pulse. The normalized profile averaged over all views is plotted (figure 7(a)) together with the greatest and least values at each point over the course of the delivery, which shows the limited extent of profile variation with angle. The ratio of the measured average profile to a reference profile is also plotted (figure 7(b)). The figure shows a tilt: tilts of 1–2% have often been seen and may either reflect changes in the beam or small sequencing inconsistencies in the (prototype) detector read-out. The read-out technique has been upgraded, but it is nonetheless sensible to make periodic checks of the lateral profile independently of the MVCT scanner. Therefore, the profile is also spot-checked each month by making ion chamber measurements of doses delivered at 5 cm deep in solid water on-axis and at ± 10 cm off-axis using a static 40×5 cm^2 field, and comparing ratios of these values to profile measurements made at commissioning.

An output stability over a typical treatment beam-on time of 5 min (check M3) is tested for a static delivery. The signal from one of the Hi-Art dose-monitoring ion chambers is used to generate a 5 min long trace of output versus time. The length of time for which a point within a patient's highly dosed target volume lies inside the borders of the Hi-Art fan beam during a helical delivery is roughly equal to the gantry period divided by the pitch—around 30 s or longer for typical clinical treatments. Therefore, the raw data shown in figure 4(b) are smoothed to generate a plot showing the variation with the time of output averaged over a 30 s window. This smoothed output should vary by less than $\pm 2\%$ around the average output of the delivery.

Uniformity of couch drive speed is tested (check M4) by taping an EDR2 film (Eastman Kodak, Rochester, NY) to the couch, marking the direction of couch drive on the film and covering the film with 15 mm of solid water build-up. With the gantry set at 0°, the film is irradiated using a 40×1 cm^2 field; the delivery takes 300 s during which time the couch is driven 20 cm. A film optical density profile along the direction of couch drive is plotted (figure 8); given a stable beam output (check M3), uniform couch speed throughout the

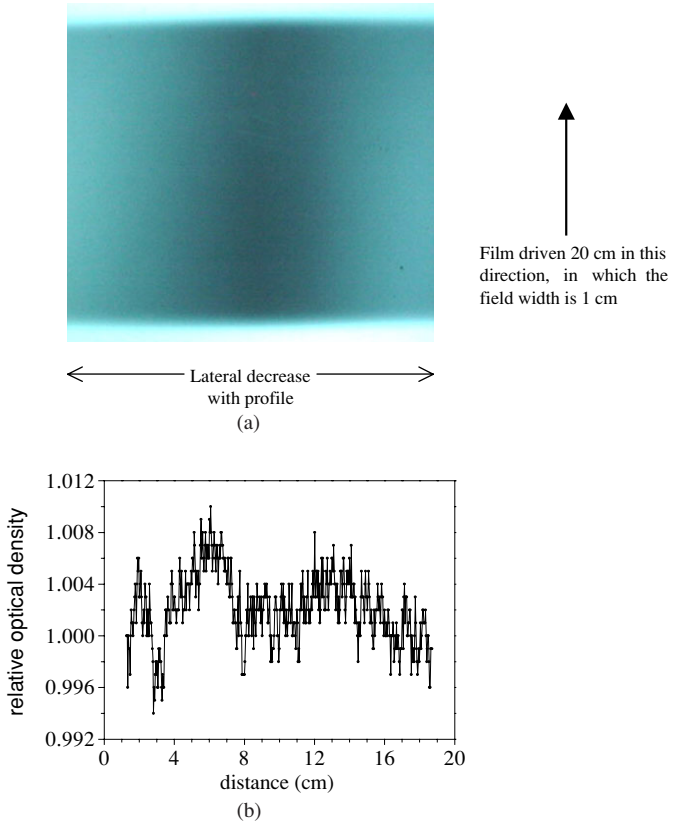

Figure 8. (a) A film irradiated using a 40 × 1 cm^2 field, to test the uniformity of couch drive speed. Optical density drops off laterally as the profile decreases, but will be uniform along the direction of couch drive if the drive speed and linac output is constant. (b) Optical density profile along a *y*-direction line running through the centre of the Hi-Art bore.

delivery will lead to a flat optical density profile (figure 8). The speed of the couch drive can conveniently be tested at the same time by placing a ZMed optical guidance system marker on the couch, and calculating the couch speed from the difference in marker positions reported by the guidance system at times towards the beginning and end of the delivery. In the absence of an optical guidance system, couch speed could simply be determined from the time taken for the couch to move between two fiducials of known separation.

To test synchrony of leaf opening and gantry angle (check M5) two Kodak X-Omat V films are placed axially (in the *x*–*z* plane) on the couch, sandwiched between slabs of solid water at ±3 cm along the *y*-axis from the virtual isocentre (figure 9). A spirit-level is used to mark a true horizontal line on each film. The films are then irradiated using a 2.5 cm wide field, opening the two middle MLC leaves for 5° projections centred on gantry angles of 0°, 120° and 240°. The gantry is rotated 40 times at a speed of 20 s per rotation, while the couch is driven 10 cm into the bore. If the delivery is adequately synchronized both films should show correctly angled star patterns (figure 10). Between irradiation of the two films the gantry rotates 24 times, and so the check will detect any possible accumulation of small offsets per rotation over the course of a typical treatment delivery.

Couch *y*-translation per gantry rotation accuracy is assessed over the course of several rotations (check M6) by taping an X-Omat V film to the couch, running the couch into and out

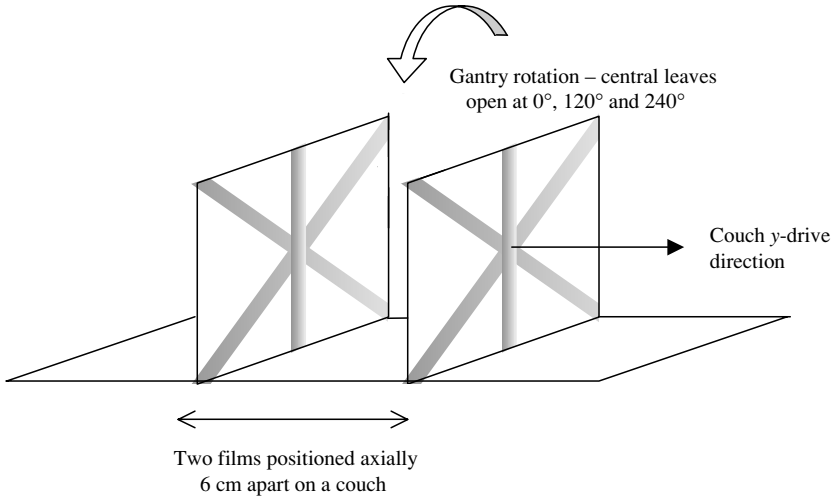

Figure 9. An illustration showing two films positioned 6 cm apart on a couch at ±3 cm from the virtual isocentre (separated by solid water slabs) to check multileaf and gantry synchrony.

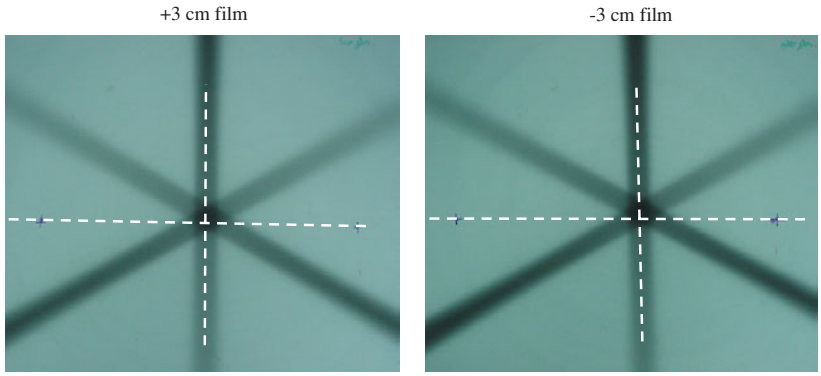

Figure 10. Two films taken to test multileaf and gantry synchrony, showing the fields planned to lie at 0°, 120° and 240° to the (marked) horizontal. The fields on both films lie within 1° of their planned angle.

of the bore and marking top laser crosshair points on the film towards its 'superior' (gantry-most) and 'inferior' edges—these marks indicating the direction of couch *y*-drive. The film is then irradiated using a 40 × 1 cm^2 field with the leaves opened for 90° segments of the 2nd, 7th and 12th of 13 rotations each of 20 s duration. The open leaf segments are centred on the 0° gantry angle, and the couch is set to drive at 1 cm per rotation (0.5 mm s^{-1}, a typical treatment velocity). The processed film is analysed to check that the peaks of the three irradiated segments lie 5 cm apart along the direction of couch drive (figure 11).

The location of the virtual isocentre (check M7) is directly tested (independently of the ZMed optical guidance system) by positioning a radiopaque marker at the reference point indicated by the lasers, taking a pair of X-Omat V films of orthogonal static 5 × 5 cm^2 fields, and checking that the marker is centred on both films. Gantry angle zero (check M8) is compared with a top (anterior/posterior) laser-defined vertical axis. The gantry is set at 0°, a film is placed on the couch and centred on the top laser crosshair, the crosshair is marked on

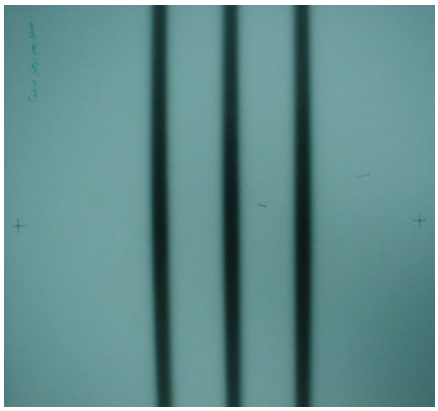

(a)

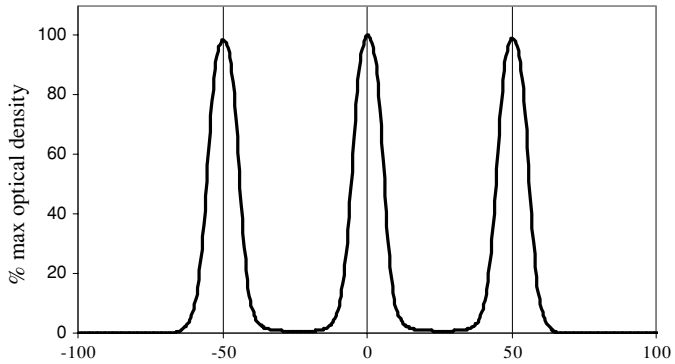

(b)

Figure 11. (a) A film irradiated to check couch and gantry synchrony over several rotations. (b) An optical density profile along the couch drive direction, showing correct (50 mm) spacing of the irradiated stripes.

the film and the film is irradiated using a 5×5 cm^2 field. Another film is taken using the same procedure but at a different couch height; if the gantry is correctly zeroed then the marked laser crosshair points will lie at the centres of the fields on both films.

Jaw width constancy (check M9) is assessed using film. The tolerance of 1 mm is tighter than that generally quoted for conventional linacs, but the specification for Hi-Art machines is actually tighter still because even a 1 mm jaw opening inaccuracy would lead to quite notable helical tomotherapy dosimetric errors (section 2.2.2.). Of course, the combined dosimetric error generated by any inaccuracy in jaw opening width, couch speed or leaf latency is tested each day using check D5. Check M9, however, provides a straightforward geometric test of field definition inaccuracy, uncoupled from other factors.

3.2.3. Three-monthly checks. Many of the three monthly checks are either standard or have been documented by Balog *et al* (2003a). Here details are provided of undocumented non-standard aspects of the three-monthly checks.

Rotational constancy of delivered dose is spot checked (T1) by positioning a 30 cm diameter solid water cylindrical phantom just beyond the edge of the treatment couch to avoid

couch attenuation, supported by two light aluminium struts. The phantom is coaxially aligned with the Hi-Art machine, and irradiated using an eight rotation delivery (field y-width of 5 cm and lateral length 2.5 cm, rotational period 20 s and no couch drive). Doses delivered to points at ± 10 cm along the x- and z-axes from the isocentre are measured with an ion chamber, and should lie in a narrow range. Rotational output stability is tested each month using check M2; however, that is a test of the stability of the *beam*, not of the *delivered dose* which outside the target region could be affected by gantry speed non-uniformity—although as linac pulsing is locked to gantry rotation, doses delivered outside the target region should be rotationally stable (section 2.2.3.).

Leaf latency (check T2) is tested as described in section 2.2.2. using the on-board MVCT detector to measure fluence when the leaves are opened. Latency data are collected for projection times between 200 and 600 ms (there being little further change as times increase beyond 600 ms), and straight lines are fitted to the resulting curves of actual versus programmed fractional opening times. These fits are compared with those obtained at commissioning and it is checked that no change of more than 2% has occurred in the fitted value of actual opening time for any particular programmed opening time.

To test for the combined effects of rotational variations in output per linac pulse and synchrony of couch drive and gantry rotation (check T3), a cylindrical solid water phantom is aligned coaxially with the Hi-Art machine and placed just beyond the end of the treatment couch, supported by aluminium struts. The phantom is comprised two hemicylinders, and between these is sandwiched an EDR2 film with a couple of points lying along the Hi-Art machine axis (indicated by a laser) marked on the film. The film is irradiated using a delivery of pitch 0.4, rotational period 20 s, helix length 15 cm, and an unmodulated fan beam of y-width 2.5 cm and lateral length 40 cm, and the on-axis film optical density y-profile is plotted (figure 12(a)). The on-axis dose-distribution should be smoothly rounded, but any rotational variation of output per pulse or gantry-couch synchrony would embed a ripple into the underlying smooth distribution, the ripple's wavelength being 1 cm for this pitch and fan beam width. Note that the on-axis film optical density profile shown in figure 8(b) (check M4), delivered using a scanned 1 cm field and measured at 15 mm depth in solid water is *not* rounded, because scanned 1 cm fields generate less rounding than scanned 2.5 cm fields and because there is less photon scatter at a depth of 15 mm than at the centre of the cylinder (Fenwick and Tomé 2004).

A smooth (quartic) curve is fitted to the central 11 cm of the on-axis profile, and the ratio of the measured optical density to the smooth fit is plotted to check for any 1 cm ripple. None is seen (figure 12(b)) which demonstrates that our Hi-Art machine is currently adequately rotationally stable, as this test can very sensitively detect such a ripple if it exists. Figures 12(c) is analogous to 12(b), but shows data measured at 10 cm off-axis where the thread effect generates a small 1 cm wavelength ripple (Kissick *et al* 2004) independently of any rotational variation of output or gantry-couch synchrony; the $\pm 2\%$ ripple is clearly seen.

Couch drive distances and directions (checks T6–8) are assessed using a mixture of film-based tests and optical guidance (again, in the absence of optical guidance, straightforward geometric fiducials can be used). A true vertical axis is established by setting up the optical guidance system to a horizontally levelled guidance array. Vertical couch drive orientation and distances can then be checked using the guidance system. Having established that the vertical couch drive is true, the orientation of the top laser can easily be tested by lining up a point on the couch to the laser crosshair, and then driving the couch up and down and checking that the crosshair remains aligned with the point.

Films of a 40×1 cm^2 field, with the couch y-drive direction marked on, are taken at gantry angles of 0° (with the film placed flat on the couch) and 90° (with the film positioned in the

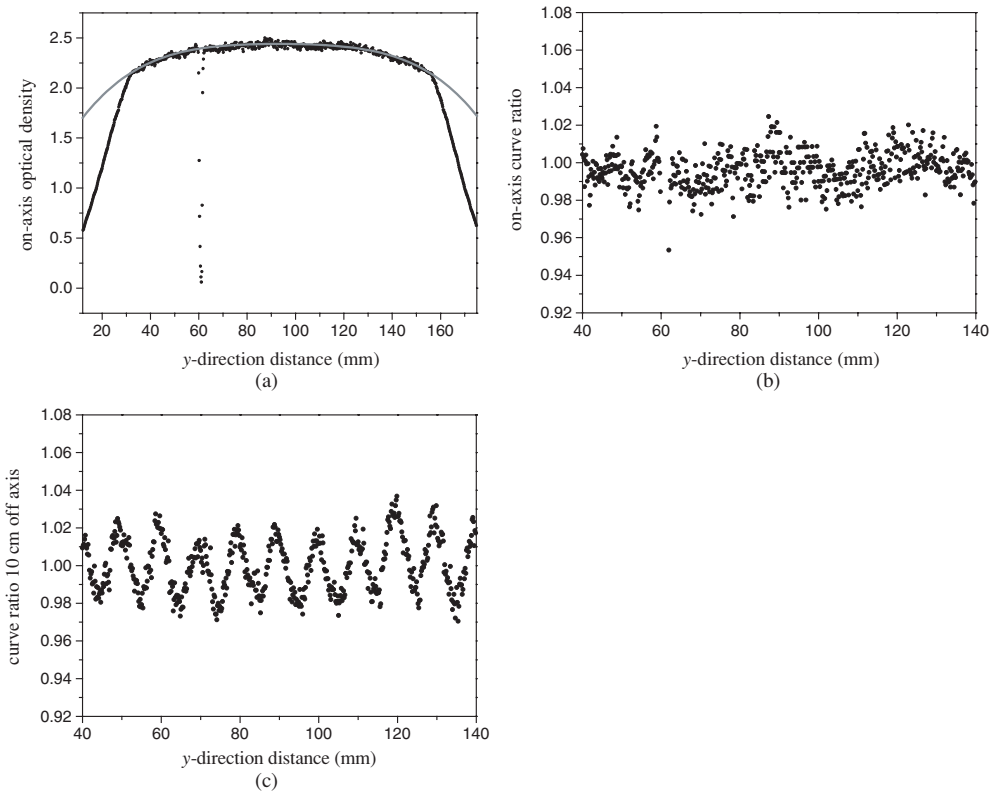

Figure 12. (a) An on-axis optical density profile is shown (black dots) together with a smooth fit (grey) to the central 11 cm of the profile, which is taken from a film that had been sandwiched between two hemicylinders coaxially aligned with the Hi-Art machine and irradiated using a 15 cm long, 2.5 cm y-width fan beam helical delivery with a pitch of 0.4. The dip at $y = 60$ cm was created by marking the Hi-Art axis on the film at that point. (b) The ratio of the on-axis measured optical density profile to the smooth fitted curve. (c) Equivalent data to that shown in figure 12(b), but measured at 10 cm off-axis, where the thread effect generates a small periodic dose variation that is clearly detected.

y–z plane) to establish that the y-drive direction is orthogonal to the gantry rotational plane—that is perpendicular to the jaws which are aligned parallel to the gantry plane. Another film, positioned in the y–z plane with the couch z- (vertical-) drive direction marked, is irradiated to check that the z-drive direction lies within the plane of the gantry—that is parallel to the jaw alignment with the gantry set to 90°. Couch drive distances in the y-direction are then tested by irradiating a film, driving the couch a set distance, irradiating again, and checking that the distance between the centres of the irradiated areas of film is that set.

3.2.4. Annual checks. Depth-dose curves and off-axis profiles are remeasured each year to ensure that they match commissioning data (check A1), work that is standardly carried out for conventional clinical accelerators (Kutcher *et al* 1994). Additionally for all jaw settings in use, a coaxially aligned cylindrical solid water phantom is helically irradiated with an unmodulated fan beam and a range of pitches and numbers of rotations (check A2). The helical delivery and phantom midplanes coincide, and doses measured at the centre of the phantom are compared to values calculated by the Hi-Art planning system. This is a sensitive test of the constancy

of the fan beam *y*-profile tails, as these determine the extent to which the dose delivered to this point rises with increasing helical delivery length (Balog *et al* 2003b, Fenwick and Tomé 2004).

Multileaf leakage (check A3) is tested by setting a jaw width of 5 cm and irradiating an X-Omat V film for 3 s with all leaves open, and then irradiating another part of the film for 300 s with all leaves closed. Given MLC leakage of less than 1%, the film darkening anywhere in the second irradiated region should be less than that at the equivalent point in the first.

Tongue-and-groove fluence effects are tested (check A4) by making fluence-per-leaf-opening measurements for various leaf opening patterns using the MVCT detector. From this data TG factors are determined (Balog *et al* 2003b) and checked against values obtained at commissioning. And lastly, output interlocking (A5) is straightforwardly tested each month by temporarily changing the reference dose-rate (held in software) and making sure that treatment deliveries interlock out after appropriate lengths of time.

4. Discussion

The QA schedule that has been developed is fairly consistent with that recommended by AAPM Topic Group 40 (Kutcher *et al* 1994) for conventional linacs. Off-axis ratio testing is far more frequent, and will remain so until the profile shape is interlocked. Rotational stability is checked more frequently than recommended by TG40, reflecting the inherently rotational nature of helical tomotherapy. The more novel components of the system (checks D4-5, M3-6, T1 and T3) are designed to test the dynamic and synchronous characteristics of Hi-Art machines. Three monthly tests may be carried out less frequently (six monthly and then annually) as more experience is gained with the machine.

This machine QA schedule has been implemented in parallel with a programme of patient-specific quality-assurance tests: detailed film and ion-chamber measurements are made in a phantom to check planned treatments before their first fraction, and *in vivo* TLD measurements are collected over the course of treatment to verify delivery. It is intended to present patient-specific QA results in another paper, together with a summary of data gathered from the machine QA programme.

In the future, delivery verification may be accomplished using dose-reconstruction software to process exit fluence data collected by the Hi-Art's MVCT detector (Kapatoes *et al* 2001a, 2001b, 2001c). While this software would provide extremely useful, detailed, automated fraction-by-fraction checking of treatment delivery, for several reasons it would complement but *not* replace the machine QA system. Firstly, by definition the dose-reconstruction software can only catch treatment errors retrospectively; thus Hi-Art machine checks should continue to be made each day before treatments commence as these will detect some problems before they lead to treatment errors.

Secondly, the software provides only an indirect inference of the dose actually delivered to a patient. Imagine the (extreme) case of a cylindrical patient aligned coaxially with the machine. Then from the exit fluence measured by the MVCT detector, it would be impossible to detect errors in couch speed or MLC/gantry synchronization—which directly impact on the absolute dose and the shape of the dose-distribution delivered to the patient, respectively. In other words, errors in these machine characteristics would only impact on exit fluence if they led to differences between planned and actual radiation path-lengths through the patient's body during treatment—requiring an irregular contour to pick them up.

Thirdly, the most effective way to monitor a machine's precise geometric set up is to directly measure the geometry; dose-reconstruction may detect some alignment errors, but would currently struggle to pick up others—for instance, jaw or multileaf twist, or beam

y-divergence. And fourthly, on those occasions when the software does detect a delivery error, machine QA records will aid assessment of whether the error is due to patient set up or a machine fault, and will likely provide an indication of which facets of machine performance might need investigation.

Similarly, machine-based and pre-treatment patient-specific QA systems are also complementary. The pre-treatment patient-specific QA work assesses the accuracy with which the planned dose-distribution is delivered to a phantom, allowing for differences between the patient's anatomy and the geometry of the phantom in which the measurements are made. While this check usefully tests all components of machine performance at once, the specific cause of any discrepancy uncovered will be diagnosed using the machine QA system, which aims to check each individual factor impacting on the delivered dose-distribution.

5. Summary

The design and dosimetric characteristics of Hi-Art machines have been reviewed. A QA system has been developed for these machines which tests both the conventional and the dynamic and synchronous aspects of Hi-Art performance. Experimental details are provided for the more novel QA tests devised, and possible future changes to the system are discussed. The complementary roles of machine QA, patient-specific pre-treatment QA and dose-reconstruction delivery verification are described. It is intended to present summaries of machine and patient-specific QA data in a future paper.

The QA system presented here builds on established conventional linac and axial tomotherapy QA methodologies, which have been modified and extended in ways that reflect the novel aspects of the Hi-Art design in the light of our experience with the machine so far. Helical tomotherapy has a relatively short clinical track record, and as further operational experience is gained it may be found that some checks should be made at different intervals to those suggested in table 1 and that additional tests need to be developed.

Acknowledgments

The authors thank the referees for most helpful and detailed reviews of this paper. John Fenwick wishes to thank the staff at Clatterbridge Centre for Oncology for teaching him how to quality assure conventional linear accelerators. This work was funded by Tomotherapy Inc and NIH grant P01 CA088960. Joshua James is supported by an AAPM/RSNA Fellowship for Graduate Study in Medical Physics.

References

Balog J, Mackie T R, Pearson D, Hui S, Paliwal B and Jeraj R 2003a Benchmarking beam alignment for a clinical helical tomotherapy device *Med. Phys.* **30** 1118–27

Balog J, Mackie T R, Reckwerdt P, Glass M and Angelos L 1999a Characterization of the output for helical delivery of intensity modulated slitbeams *Med. Phys.* **26** 55–64

Balog J, Mackie T R, Wenman D L, Glass M, Fang G and Pearson D 1999b Multileaf collimator interleaf transmission *Med. Phys.* **26** 176–86

Balog J, Olivera G and Kapatoes J 2003b Clinical helical tomotherapy commissioning dosimetry *Med. Phys.* **30** 3097–106

Chaney E L, Cullip T J and Gabriel T A 1994 A Monte Carlo study of accelerator head scatter *Med. Phys.* **21** 1383–90

Deasy J O, Fowler J F, Roti J L and Low D A 2001 Dose-rate effects in intensity modulated radiation therapy *Int. J. Radiat. Oncol. Biol. Phys.* **51 S1** 400–1

Fenwick J D and Tomé W A 2004 Modelling simple helically-delivered dose-distributions *Phys. Med. Biol.* submitted

IEC 1996 *Report 1217—Guide to Coordinates, Movements and Scales used for Radiotherapy Equipment* BS EN 61217 (London: BSI)

Kalender W A and Polacin A 1991 Physical performance characteristics of spiral CT scanning *Med. Phys.* **18** 910–5

Kapatoes J M, Olivera G H, Balog J P, Keller H, Reckwerdt P J and Mackie T R 2001a On the accuracy and effectiveness of dose reconstruction for tomotherapy *Phys. Med. Biol.* **46** 943–66

Kapatoes J M, Olivera G H, Ruchala K J and Mackie T R 2001b On the verification of the incident fluence in tomotherapy IMRT *Phys. Med. Biol.* **46** 2953–63

Kapatoes J M, Olivera G H, Ruchala K J, Smilowitz J B, Reckwerdt P J and Mackie T R 2001c A feasible method for clinical delivery verification and dose reconstruction in tomotherapy *Med. Phys.* **28** 528–42

Kissick M W, Fenwick J D, Jeraj R, Kapatoes J M, Keller H and Mackie T R 2004 The helical tomotherapy thread effect *Med. Phys.* submitted

Kutcher G J, Coia L, Gillin M, Hanson W F, Leibel S, Morton R J, Palta J R, Purdy J A, Reinstein L E, Svensson G K, Weller M and Wingfield L 1994 Comprehensive QA for radiation oncology: report of AAPM Radiation Therapy Committee Task Group 40 *Med. Phys.* **21** 581–618

LoSasso T, Chui C-S and Ling C C 1998 Physical and dosimetric aspects of a multileaf collimator system used in the dynamic mode for implementing intensity modulated radiotherapy *Med. Phys.* **25** 1919–27

Low D A, Chao K S C, Mutic S, Gerber R L, Perez C A and Purdy J A 1998a Quality assurance of serial tomotherapy for head and neck treatments *Int. J. Radiat. Oncol. Biol. Phys.* **42** 681–92

Low D A, Mutic S, Dempsey J F, Gerber R L, Bosch W R, Perez C A and Purdy J A 1998b Quantitative dosimetric verification of an IMRT planning and delivery system *Radiother. Oncol.* **49** 305–16

Low D A, Mutic S, Dempsey J F, Markman J, Goddu S M and Purdy J A 1999 Abutment region dosimetry for serial tomotherapy *Int. J. Radiat. Oncol. Biol. Phys.* **45** 193–203

Mackie T R, Balog J, Ruchala K, Shepard D, Aldridge J S, Fitchard E E, Reckwerdt P, Olivera G H, McNutt T and Mehta M 1999 Tomotherapy *Semin. Radiat. Oncol.* **9** 108–17

Mackie T R, Holmes T, Swerdloff S, Reckwerdt P, Deasy J O, Yang J, Paliwal B and Kinsella T 1993 Tomotherapy: a new concept for the delivery of dynamic conformal radiotherapy *Med. Phys.* **20** 1709–19

Reckwerdt P J, Olivera G H, Shepard D M and Mackie T R 2000 Case studies in tomotherapy optimization: breast, prostate, mesothelioma and nasopharyngeal treatments *Proc. 13th Int. Conf. on the Use of Computers in Radiation Therapy (Heidelberg, May 2000)* ed W Schlegel and T Bortfeld (Heidelberg: Springer) pp 60–2

Tsai J-S, Rivard M J and Engler M J 2000 Dependence of linac output on the switch rate of an intensity-modulated tomotherapy collimator *Med. Phys.* **27** 2215–25

Woo S Y, Grant W, McGary J E, Teh B S and Butler E B 2003 The evolution of quality assurance for intensity-modulated radiation therapy (IMRT): sequential tomotherapy *Int. J. Radiat. Oncol. Biol. Phys.* **56** 274–86